

NON-LINEAR EFFECTS FOR FREQUENCY TUNING AND QUADRATURE COMPENSATION OF A PZT SELF-CALIBRATION COMPATIBLE Z-AXIS GYROSCOPE

Sachin Nadig, Visarute Pinrod, and Amit Lal

SonicMEMS Laboratory, School of Electrical and Computer Engineering
Cornell University, Ithaca, NY, USA

ABSTRACT

This work presents frequency tuning and quadrature cancellation of a bulk-PZT gyroscope. We leverage non-linearity of elasticity and piezoelectric coupling in lateral PZT bimorphs for frequency and quadrature tuning. Frequency and quadrature tuning is demonstrated with an applied DC voltage, as a broadband control for potential closed loop operation. Resonance and quadrature tuning of $\sim 10\text{ppm}/V_{dc}$ and $20\text{deg/sec}/V_{dc}$ respectively were achieved using non-linear operation of PZT drive and sense resonators at $10V_{peak} \sim 108\text{ kHz}$ drive.

INTRODUCTION

Piezoelectric transduction has been an attractive choice for gyroscopes owing to their high electromechanical coupling coefficients (k_c^2) of some piezoelectric materials compared to that of capacitive gyroscopes [1]. Piezoelectric gyroscopes of different form factors, design and material choices have been explored. Although, some of the previous works have demonstrated good sensitivity and quality factors [1,2] the solutions have often been of large form factors and not planar in design. The quartz tuning fork gyroscope demonstrated in [1] relies on side wall electrodes which could be difficult to fabricate at smaller scales. Planar shear mode gyroscopes [3] and SAW gyroscopes [4] offer high shock survivability, often a desirable metric for inertial sensors in industrial applications, however have so far suffered from low sensitivities. Recently, thin film AlN on silicon BAW gyroscope in [5] demonstrated a planar design with good sensitivity and shock tolerance. Alternatively, a bulk-PZT gyroscope was demonstrated in [6] with high sensitivity owing to its high electromechanical coupling coefficients. The higher aspect ratio in bulk-PZT gyroscope enabled gap-free sensors with high dynamic range and better shock tolerance. Additionally, the potential for monolithic integration of bulk-PZT gyroscope onto precision piezoelectric in-situ calibration platforms [7] using the laser micromachining process, makes it a desirable candidate for high performance gyroscopes.

As in most gyroscopes, fabrication variation often leads to non-ideal spring constants causing frequency mismatch and cross-axis stiffness components between drive and sense [8]. These errors prove to be detrimental for gyroscope operation as they lead to bias and quadrature errors [8]. Also, the resonance frequency is known to drift with temperature and aging, especially in PZT [1, 9] leading to variability in scale-factor and bias, which are sources of instabilities. Operating under closed loop with mode-matched drive and sense resonance, along with quadrature control is one of the pathways for high

performance gyroscopes [8]. Previous work on piezoelectric gyroscope tuning and controls has focused on electrostatic tuning mechanisms [10]. However, this technique still relies on micro-scale gaps, making it susceptible to failure under high shock conditions and limited sensor dynamic range. Recent work in gap free piezoelectric tuning schemes [5] has shown AC tuning of resonance frequency for AlN on silicon BAW gyroscopes. In this work, piezoelectric tuning of frequency and quadrature error in bulk-PZT gyroscope with DC voltages is presented. This approach circumvents the problems of feedthrough and phase errors that arise in AC tuning methods.

BULK PZT GYROSCOPE

Design

The bulk-PZT gyroscope design demonstrated in this work is a Coriolis vibratory yaw rate gyroscope. As described in [6] the device is a single mass sensor with 8 lateral PZT bimorphs, each with 2 electrodes. The entire device is made of bulk PZT-4. Figure 1 shows the device schematic with all the lateral bimorph labelled. D3 and D4 are connected to have a fully-differential piezoelectric drive (*Drv*). Additionally, they also allow for drive resonator frequency tune. Similarly, S1 and S2 are used to measure sense resonator characteristics (*Sdrv*). Coriolis signal is detected on the differential sense bimorph S4 (*Sns*). The design also allows for dedicated bimorphs for tuning out fabrication and aging induced errors. Lateral bimorph (*Dpf*) is used for sensing drive resonance. The differential signal from this drive resonance pick-off bimorph is used in the feedback control of the drive resonator frequency and amplitude. Using the combination of bimorphs D2 and S3, we can tune for quadrature (k_{xy}) errors using *Qtn1* and *Qtn2*. The tuning of k_x , k_y and k_{xy} is possible by virtue of non-linear drive.

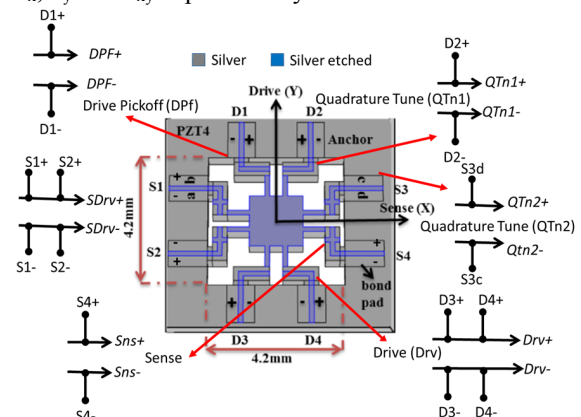


Figure 1: PZT-gyro schematic showing drive, sense and electrodes for frequency and quadrature tune

As described in [11], for a generic vibratory gyroscope, the errors in our gyroscope leading to mode split can be modelled as mismatches in the stiffness in the drive and sense resonators (k_x , k_y). Additionally, cross-axis stiffness (k_{xy}) arises from fabrication intolerance and spring non-idealities. For mode-matching our gyroscope we need to tune for k_x , k_y and also k_{xy} . Closed loop control of errors is necessary as the frequency and damping mismatches are often changing with time and temperature. We explored ways to tune out such errors electronically, with dedicated loop controls for drive and sense resonators and quadrature control. Here, we show sensitivities of frequency and quadrature tuning loops.

Device Non-linearity

Our gyroscope utilizes the piezoelectric properties of PZT lateral bimorph in actuator and sensor designs. In PZT, material properties such as Young's modulus, d-coefficients, dielectric constants and mechanical loss factor have non-linear dependence to stress [12]. A simple model of a spring-mass piezoelectric resonator can be expressed as,

$$\ddot{x} + \alpha\dot{x} + \omega_0^2 x = F \cos(\Omega t) \quad (1)$$

Where, α is the mass normalized viscous damping, F is the amplitude of the piezoelectric force, Ω is the applied force frequency and ω_0 is the natural frequency of the resonator. Resonant frequency of a resonator is proportional to the Young's modulus (E) and elasticity in general.

$$\omega_0^2 \propto \frac{Ewh^3}{4l^3m} \quad (2)$$

Where, m is the mass. The non-linearity in E due to stress in PZT can be expressed as [12],

$$E = E_0 + \beta E_0 T_m^2 + (\text{higher order terms}) \quad (3)$$

Where, $\beta = \Delta E / E_0$ and T_m is the stress

The stress caused due to piezoelectric drive is,

$$T_m = T_0 \cos(\Omega t + \phi) + T_{dc} \quad (4)$$

$$T_0 \propto \frac{d_{31}V_{ac}}{h} \quad (5)$$

Where, T_{dc} is the stress caused by DC voltage. Combining equations (1)-(5), an approximate model of the non-linear resonator can be expressed as,

$$\begin{aligned} \ddot{x} + \alpha\dot{x} + \omega_0^2 \left[1 + \beta \left(\frac{T_0^2}{2} + T_{dc}^2 \right) \right] x + \\ \omega_0^2 \left[\beta \left(2T_{dc}T_0 \cos(\Omega t + \phi) + \frac{T_0^2}{2} \cos(2\Omega t + 2\phi) + \dots \right) \right] x \\ = F \cos(\Omega t) \end{aligned} \quad (6)$$

Non-linearity in the elastic constants can be leveraged by operating the resonator at high stress regions (stresses $> 10^7$ Pa) [12]. As shown in (6), we can use the stress induced by DC voltage to bias the resonator at different small signal stiffness. The non-linearity in E also leads to higher order harmonics in the resonator response. DC control of stress for bimorphs in the drive (D3, D4) and sense resonator (S1, S2) tunes k_y , k_x for mode matching purposes. Additionally, by having a DC control of stress

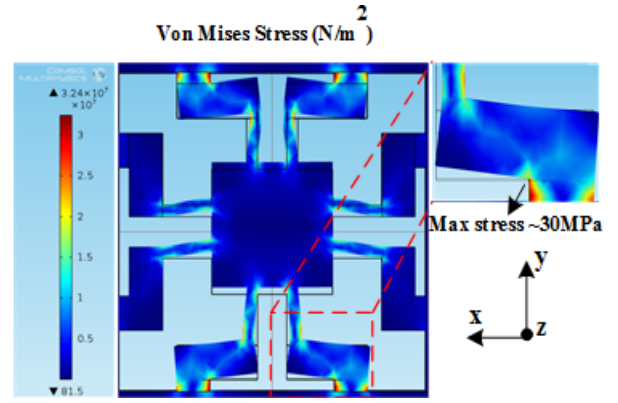


Figure 2: COSMOL simulation showing Von Mises stress for 10V drive at resonance.

on D2 and S3 bimorphs, we can tune for quadrature error by controlling off-diagonal spring constant of the resonator (k_{xy}).

Using finite element analysis software (COMSOL), we simulated the stress as a function of drive voltage in our piezoelectric gyroscope. This was done to calculate the drive voltage required to operate in the non-linear region. COMSOL simulation in Figure 2 shows the stress distribution for our device. Simulation predicted that for our design, the Von-Mises stress was $>10^7$ Pa ($<$ yield stress ~ 500 MPa for PZT) for 10V drive at resonance. With stress higher than 10^7 Pa, we can be certain that non-linearity can be achieved for $\geq 10V_{peak}$ drive

Fabrication

The device was fabricated using laser micromachining process described in [6]. Thick bulk PZT plates (500 micron thick) with silver electrodes on both top and bottom were laser micro-machined. High aspect ratio (width: height of 3:10) with reduced side wall angles were achieved by repetitive hatching of dense laser scan lines. Post fabrication, the device is bonded onto a custom PCB with a silver acrylic and wire bonded. For further testing and characterization, we designed an interface PCB for controls. PZT-gyroscope is operated in air, packaged on a custom PCB and connected to interface electronics for characterization as shown in Figure 3.

Gyroscope Interface and Controls

Figure 4 shows the schematic of gyroscope control PCB. Zurich Instrument HF2LI is used for frequency response measurements, synchronous demodulation, PID and PLL control loops. The interface circuit for the gyroscope was designed using off the shelf components. The gyroscope drive circuit has two high voltage operational amplifiers (Apex Microelectronics PA443DF). High voltage amplifiers (PiezoDrive PDM200B) were used to amplify (x20) precision DC tune voltage (0-5V), up to $\pm 150V$ and added to the AC drive from HF2LI. Similar drive is used for S_{drv} while measuring sense resonator response. In the sense circuit, TL082 JFET opamps with $1M\Omega$ resistors buffer output from S_{ns} to HF2LI. In the quadrature tuning, PA443DF amplifies (x20) DC tune voltages, and provides bridge drive to Q_{tn1} and Q_{tn2} . An external power source supplies $\pm 12V$ to the PCB.

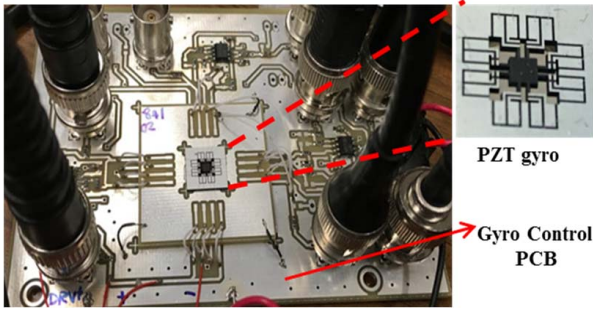


Figure 3: Fabricated device bonded using silver acrylic onto PCB with control electronics and interface to Zurich Instruments HF2li

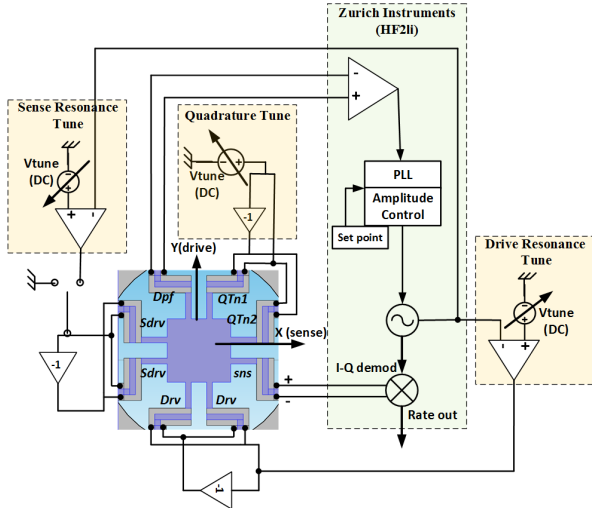


Figure 4: Interface circuit schematic for frequency tuning and quadrature compensation with DC tuning voltages

RESULTS

Gyroscope frequency response

Using Zurich Instruments lock in amplifier (HF2li), we measured the frequency response of our device for $10V_{\text{peak}}$ differential drive on the *Drv* and *Sdrv* electrodes. The frequency response of the device for the Y (drive) and X (sense) resonators is shown in figure 5. The resonator has a quality factor (Q) ~ 100 , electromechanical coupling factor (k_t^2) $\sim 12\%$ with drive resonance frequency ~ 108 kHz. Frequency domain analysis in COMSOL, under symmetric meshing conditions yielded the resonance mode to within 5% of the experimental results. The mode shapes of the drive and sense simulated using COMSOL is as shown in the inset of figure 5. The model here does not include damping and spring constant mismatches. Without any tuning, the device shown had a mode split of <80 Hz. Several other devices were characterized for the as-fabricated mode splits. Although the devices were symmetric in design, most devices had <100 Hz mode split owing to the fabrication inaccuracies arising from the laser micromachining process.

Non-linear resonator response

In order to operate the gyroscope in the non-linear regime, we drive our device at $10V_{\text{peak}}$ at resonance. The tuning voltages were all set to zero for measuring the non-linear response of the drive resonator.

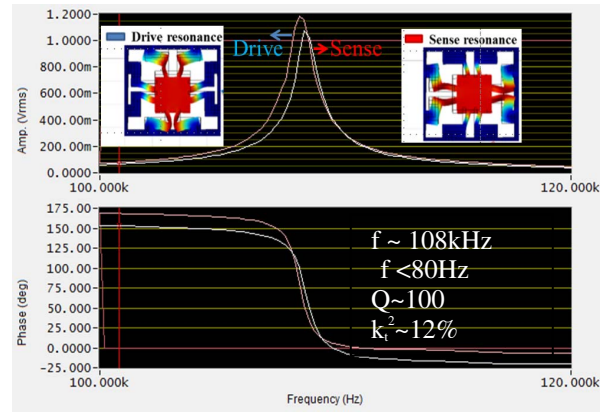


Figure 5: Measured frequency response of the drive and sense resonators. As-fabricated mode split < 80 Hz. Inset shows COMSOL mode simulations for drive and sense resonance

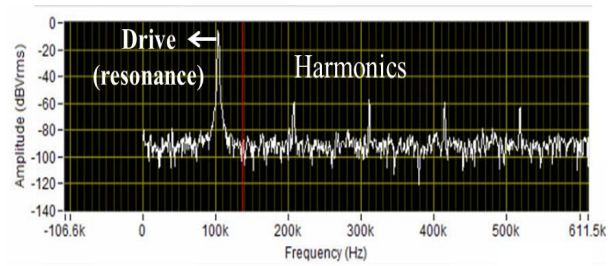


Figure 6: Resonator non-linearity: Frequency response of drive pick-off electrode (*Dpf*) on $10V$ drive (*Drv*) at resonance. Non-linear dependence of elasticity to stress in PZT allows for tuning of spring constants

Further, the gyroscope is operated under closed loop drive conditions using phase locked loop (PLL) and fixed drive amplitude using proportional control for optimal operation [8]. Figure 6 shows the frequency response of differential signals obtained from *Dpf* bimorph. We measured the drive resonator to have higher order harmonics. However, we observed that any harmonics for $<10V_{\text{peak}}$ drive were not measurable. As suggested by our simulation result in figure 2, we see non-linearity for drive $\geq 10V_{\text{peak}}$ at resonance, when the high stress criterion is met.

Resonance frequency tuning

The gyroscope is operated under closed loop non-linear drive conditions as explained before. The drive signals are frequency controlled using phased locked loop to track the resonance frequency shifts. An additional DC voltage on the drive electrodes (*Drv*), changes the resonance frequency of the drive resonator. Figure 7 shows the frequency shifts recorded using PLL for manual sweep of DC voltages on *Drv* electrodes. On applying $50V_{\text{dc}}$, the drive resonator frequency shifted by 50 Hz from its initial resonance frequency of ~ 108 kHz. We measured the frequency tune sensitivity of DC voltage to be $\sim 10\text{ppm}/V_{\text{dc}}$.

Quadrature tuning

To demonstrate quadrature tuning sensitivity of DC voltages on *Qtn* electrodes, the gyroscope was operated

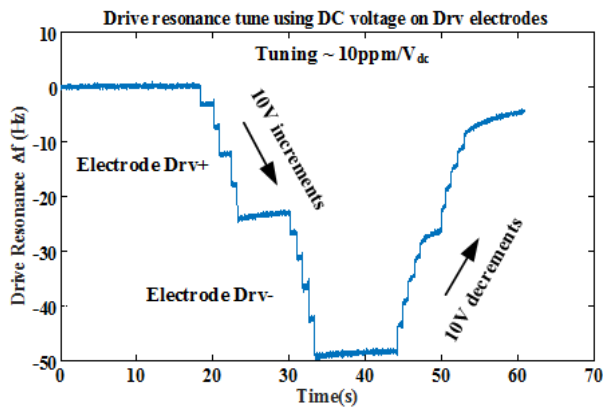


Figure 7: Frequency tuning sensitivity: Change in the drive resonance frequency with DC voltages on Drv electrodes under closed loop drive operation, measured by the HF2li lock-in amplifier PLL

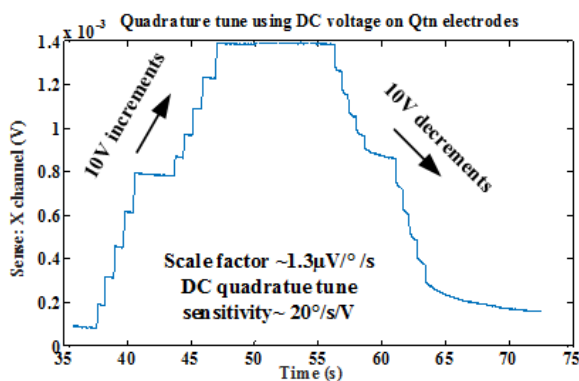


Figure 8: DC voltage quadrature tune sensitivity: Initial quadrature is removed using AC voltages at resonance on Sdrv electrodes. Plot shows quadrature tuning sensitivity for DC voltage sweep on QTn electrodes under closed loop drive operation

under the closed loop drive condition as described above. The sense resonator was operated under open loop and the output was obtained by synchronous demodulation at the drive resonance frequency. The gyroscope was operated under mode-mismatched condition with demodulation phase correction ($\sim 15^\circ$) due to the mode-split. Initial quadrature was cancelled using AC voltages on Sdrv to record the effect of DC quadrature tune. Effect of DC voltage on quadrature is shown in Figure 8 to demonstrate k_{xy} compensation. In our experiments, the DC voltages were swept manually, in 10V increments while recording the quadrature channel. For a scale factor of $1.3\mu\text{V}/\text{deg/s}$ [6], we measure a quadrature tune sensitivity of $\sim 20\text{deg/s}/V_{dc}$.

CONCLUSION

A bulk PZT gyroscope with non-linear properties was designed, fabricated and characterized. We have developed a design with DC voltages as control knobs on a PZT gyroscope to adjust the spring constants and resonance frequencies to actively tune gyroscope scale factor and bias. We demonstrated resonance frequency tuning and quadrature compensation with DC voltages. The tuning sensitivities were $10\text{ppm}/V_{dc}$ and $20\text{deg/s}/V_{dc}$ respectively. Under closed loop operation, with active tuning, dynamic mode-matching of piezoelectric

gyroscopes can be made possible. The gyroscope operation and tune technique is invariant to gaps, unlike electrostatic counterparts, making it a potential candidate for high shock applications. Monolithic integration of PZT gyroscope onto PZT calibration stage enables a complete solution for continuous scale factor and bias calibration.

ACKNOWLEDGEMENTS

We would like to thank DARPA PASCAL program for funding this work. This work was performed in part at the Cornell Nano Scale Facility, a member of the National Nanotechnology Infrastructure Network, which is supported by the National Science Foundation (Grant ECCS-0335765).

REFERENCE

- [1] Söderkvist, Jan. "Micromachined gyroscopes." *Sensors and Actuators A: Physical* 43.1 (1994): 65-71.
- [2] Ono, Keisuke, Masanori Yachi, and Noboru Wakatsuki. "H-type single crystal piezoelectric gyroscope of an oppositely polarized LiNbO₃ plate." *Japanese Journal of Applied Physics* 40.5S (2001): 3699.
- [3] Maenaka, K., et al. "Novel solid micro-gyroscope." *19th IEEE International Conference on Micro Electro Mechanical Systems*. IEEE, 2006.
- [4] Jose, K. A., et al. "Surface acoustic wave MEMS gyroscope." *Wave motion* 36.4 (2002): 367-381.
- [5] Hodjat-Shamami, Mojtaba, et al. "A dynamically mode-matched piezoelectrically transduced high-frequency flexural disk gyroscope." *2015 28th IEEE International Conference on Micro Electro Mechanical Systems (MEMS)*. IEEE, 2015.
- [6] Nadig, Sachin, Serhan Ardanuç, and Amit Lal. "Self-calibration compatible Z-axis bulk PZT vibratory gyroscope." *2015 Transducers-2015 18th International Conference on Solid-State Sensors, Actuators and Microsystems (TRANSDUCERS)*. IEEE, 2015.
- [7] Nadig, Sachin, et al. "Multi-modal mechanical stimuli stage for in-situ calibration of MEMS gyroscopes." *Inertial Sensors and Systems (ISSS), 2015 IEEE International Symposium on*. IEEE, 2015.
- [8] Sharma, Ajit, et al. "A 0.1/HR bias drift electronically matched tuning fork microgyroscope." *Micro Electro Mechanical Systems, 2008. MEMS 2008. IEEE 21st International Conference on*. IEEE, 2008.
- [9] Genenko, Yuri A., et al. "Mechanisms of aging and fatigue in ferroelectrics." *Materials Science and Engineering: B* 192 (2015): 52-82.
- [10] Elsayed, Mohannad Y., et al. "Bulk Mode Disk Resonator With Transverse Piezoelectric Actuation and Electrostatic Tuning." *Journal of Microelectromechanical Systems* 25.2 (2016): 252-261.
- [11] Lynch, D. D. "Vibratory gyro analysis by the method of averaging." *Proc. 2nd St. Petersburg Conf. on Gyroscopic Technology and Navigation, St. Petersburg*. 1995.
- [12] Pérez, Rafel, et al. "Extrinsic contribution to the non-linearity in a PZT disc." *Journal of Physics D: Applied Physics* 37.19 (2004): 2648.